Soft Matter

Phase behavior and design rules for plastic colloidal crystals of hard polyhedra via consideration of directional entropic forces

Journal:	*Soft Matter*
Manuscript ID	SM-ART-12-2018-002643.R1
Article Type:	Paper
Date Submitted by the Author:	02-May-2019
Complete List of Authors:	Karas, Andrew; University of Michigan, Chemical Engineering Dshemuchadse, Julia; University of Michigan, Department of Chemical Engineering van Anders, Greg; University of Michigan, Chemical Engineering Glotzer, Sharon; University of Michigan, Chemical Engineering

Journal Name

ARTICLE TYPE

Cite this: DOI: 10.1039/xxxxxxxxxx

Phase behavior and design rules for plastic colloidal crystals of hard polyhedra via consideration of directional entropic forces†

Andrew S. Karas,[a] Julia Dshemuchadse,[a] Greg van Anders,[b] and Sharon C. Glotzer*[a,c,d]

Received Date
Accepted Date

DOI: 10.1039/xxxxxxxxxx

www.rsc.org/journalname

Plastic crystals — like liquid crystals — are mesophases that can exist between liquids and crystals and possess some of the characteristic traits of each of these states of matter. Plastic crystals exhibit translational order but orientational disorder. Here, we characterize the phase behavior in systems of hard polyhedra that self-assemble plastic face-centered cubic (pFCC) colloidal crystals. We report a first-order transition from a pFCC to a body-centered tetragonal (BCT) crystal, a smooth crossover from pFCC to an orientationally-ordered FCC crystal, and an apparent orientational glass transition wherein long-range order fails to develop from a plastic crystal upon an increase in density. Using global order parameters and local environment descriptors, we describe how particle shape influences the development of orientational order with increasing density, and we provide design rules based on the arrangement of facets for engineering plastic crystal behavior in colloidal systems.

1 Introduction

Anisotropic molecules and particles are known to exhibit two types of thermodynamically stable mesophases between a liquid and a crystal: the liquid crystal and the plastic crystal (PC). The liquid crystal phase, in which particles have orientational order but lack long-range translational order, has been thoroughly studied for many kinds of systems[1–3]. Much less is known about the plastic crystal, in which particles have translational order but lack long-range orientational order. Our understanding of plastic crystals originates from observations of molecular systems. In 1930, Pauling presented a statistical mechanics argument explaining how molecules in a crystalline phase could undergo a transition from oscillatory motion to rotational motion as a way to explain temperature-dependent phenomena in thermodynamic properties[4]. Timmermans later coined the term 'plastic crystal' to describe phases formed by globular compounds that are far easier to deform than lower-temperature phases[5]. These plastic crystal phases typically have cubic symmetry, they lead to a significantly lower entropy of melting as compared to non-globular compounds, and they can form within many different organic or inorganic systems[6,7]. It is also possible to quench a plastic crystal into an orientational glass wherein the system maintains a higher-symmetry unit cell, rotational motion slows as the system vitrifies, and long-range orientational order is absent[8–11].

Entropic plastic crystals have recently been reported in systems of nanoparticles[12,13] and in computer simulations of hard particles[14–20]. Existing literature on Monte Carlo simulations shows that hard particle plastic crystals are a thermodynamic state distinct from the orientationally ordered crystal phase[14,18], that plastic crystals are typically formed by spheroidal particles[14,15,18], that the existence of a plastic crystal phase lowers the free energy barrier for crystallization from a fluid[19], and that particle orientations in the plastic crystal phase are not random but rather some orientations are more likely to occur than others[18–21]. The recent development of the theory of directional entropic forces (DEFs)[22,23] and the quantification of these forces through the potential of mean force and torque (PMFT)[24] provide a new approach to the analysis of plastic crystal systems.

Here we describe how particle shape impacts the development of orientational order in hard particle systems that form plastic face-centered cubic (pFCC) crystals. We develop new techniques that allow us to characterize the orientational coupling in orientationally ordered and disordered states. We study four shapes that all form pFCC crystals, but exhibit different plastic-crystal-to-crystal transitions: first-order phase transitions, continuous orientational order development without a thermodynamic phase transition, and an approach to an orientational glass transition where

[a] Department of Chemical Engineering, University of Michigan, Ann Arbor, MI 48109, USA
[a] Department of Physics, University of Michigan, Ann Arbor, MI 48109, USA
[c] Department of Materials Science and Engineering, University of Michigan, Ann Arbor, MI 48109, USA
[d] Biointerfaces Institute, University of Michigan, Ann Arbor, MI 48109, USA. Email: sglotzer@umich.edu

† Electronic Supplementary Information (ESI) available: see DOI: 10.1039/b000000x/

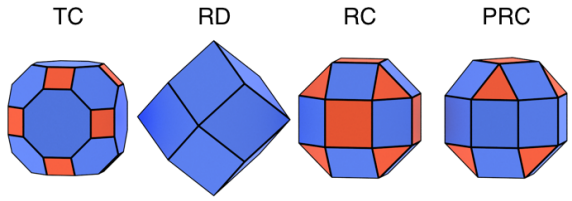

Fig. 1 The four shapes used in the study: Truncated Cuboctahedron (TC), Rhombic Dodecahedron (RD), Rhombicuboctahedron (RC), and Pseudorhombicuboctahedron (PRC). We are able to identify that some polyhedral facets are more important than others in dictating how neighbors align with respect to one another: the facets with the strongest directional entropic forces are shown in blue, and the remaining facets are colored red.

there is no phase transition or long-range orientational order. In particular, we compare how shape features relative to that of the rhombicuboctahedron affect the development of orientational order. Fig. 1 shows the shapes investigated and Fig. 2 shows the phases that they form. We develop an order parameter based on the similarity of particle orientations within a system as compared to those of a perfect crystal. The order parameter captures the discontinuous change in orientational order across a first-order transition for shapes of arbitrary symmetry. We characterize the local environments of particles by calculating the potential of mean force and torque (PMFT)[24] and orientation-orientation correlations between a reference particle and its neighbors. Through this analysis, we identify relationships between shape features and plastic crystalline behavior. Specifically, we show that the arrangement of the largest facets and the ensuing DEFs dictate how orientational order develops. We conclude with general design rules for engineering PC behavior in colloidal crystals.

2 Model and Methods

We study four shapes that are all known to self-assemble FCC crystals:[15] the truncated cuboctahedron (TC), rhombic dodecahedron (RD), rhombicuboctahedron (RC), and pseudorhombicuboctahedron (PRC; also known as the elongated square gyrobicupola). Particle shapes are depicted in Fig. 1 with the most impactful facets – from a DEF standpoint – colored blue. How the shapes differ from the RC is found to be important in determining the behavior of these systems. The RC is a shape with 26 facets, 12 of which are square facets that align with the nearest-neighbor directions of the FCC crystal (*i.e.*, the coordination geometry). The TC has the same number of facets and their normal vectors point in the same direction as those of the RC, but the larger facets of the TC — six octagonal and eight hexagonal ones — do not align with the FCC coordination geometry. The RD is the Voronoi particle of FCC, and thus tiles space. All 12 facets of the RD align with the FCC environment. Lastly, the PRC has the same types of facets as the RC, but they are arranged differently, resulting in a reduced, tetragonal symmetry. One can construct the PRC from the RC by taking a square cupola portion of the RC and rotating it by 45°. While the RC has a set of 12 square facets that align with FCC coordination geometry, only eight square facets of PRC can align at a given time.

We use several techniques to investigate the behavior of plastic crystals and their phase transitions. We perform all simulations with the hard particle Monte Carlo (HPMC) package of HOOMD-blue[25–27]. We compute the equation of state as the primary indicator of phase behavior. Systems with $N = 864$ particles were simulated in a "floppy-box" *NVT* ensemble, where the volume is kept constant while allowing for box shearing and changes in box aspect ratios[28]. We compute pressure *via* the scale distribution function (SDF) in HPMC[27]. We present data using the reduced pressure $p^* = \beta p v_0$ where $\beta = (k_B T)^{-1}$ and v_0 is particle volume. For all shapes, v_0 is set to 1.0 such that system density is equivalent to packing fraction. For simulation trajectories used when calculating local environment descriptors, we use system sizes $N = 2048$. For the TC and RC, we run additional simulations with system sizes between $N = 256$ and $N = 16384$ in order (*i*) to show system-size dependent changes indicating a first-order transition for the TC and (*ii*) to show that there is no system-size dependence on the bulk modulus for the RC. For the TC, we additionally validate the first-order transition through *NPT* simulations for systems of $N = 2048$ to test for the presence of hysteresis. Data were collected by both compressing the system from a pFCC crystal and expanding the system from a dense crystal. For expansion simulations, we initialize particles in orientationally ordered structures that result from compression of the plastic crystal; an FCC lattice for RC and RD, and a BCT lattice for TC and PRC.

We quantify global orientational order by measuring the orientation of particles relative to global reference orientations. If we represent particle orientations as quaternions, the difference in orientation between a particle described by an orientation q_0 to a reference orientation q_{ref} is given by

$$Q_{net} = q_{\text{ref}}^{\dagger} q_0 = \exp(\frac{i}{2}\theta\hat{n}\cdot\vec{\sigma}) = \cos(\frac{\theta}{2}) + i\hat{n}\cdot\vec{\sigma}\sin(\frac{\theta}{2}) , \quad (1)$$

where we use Pauli matrices $\vec{\sigma}$ to give an explicit representation of the rotation of an angle θ in a plane perpendicular to $\hat{n}$. The trace of $\frac{1}{2}\text{Tr}(Q_{net})$ is a global rotational invariant with values between -1 and 1.

To construct the order parameter, we first select a set of q_{ref} from a set of j quaternions corresponding to orientations found in the dense, orientationally ordered crystal ($j = 1$ for RD and RC, and $j = 2$ for TC and PRC). Next, we determine the average $\text{Tr}(Q_{net})$ for a randomly oriented particle, which we denote by Ψ_r, by integrating over the group manifold of SO(3) *modulo* the particle's point group symmetry Γ,

$$\Psi_r = \frac{1}{2}\int_{\text{SO(3)}/\Gamma} dq \max_j \text{Tr}(q_{\text{ref},j}^{\dagger} q). \quad (2)$$

For simplicity, we compute Ψ_r *via* Monte Carlo integration by sampling 500,000 random quaternions. We compare Ψ_r against the quantity

$$\Psi_s = \frac{1}{2N}\sum_i^N \max_j \text{Tr}(q_{\text{ref},j}^{\dagger} q_i) , \quad (3)$$

which we measure when simulating dense systems of shapes.

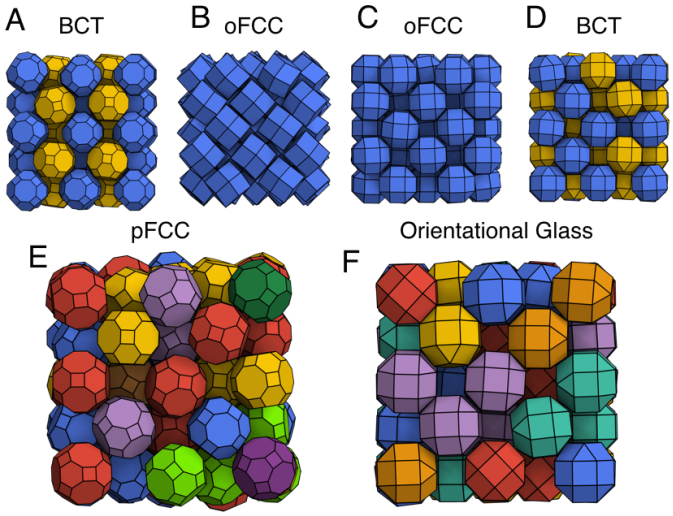

Fig. 2 Representative images of different phases studied in this work, with particles colored based on their orientation. *(A–D)* The high-density phase for each shape. *(A)* TC form BCT crystals upon compression of the pFCC. *(B & C)* RD and RC maintain FCC order, but they develop strong orientational order and exist in this ordered FCC (oFCC) at high density. *(D)* PRC can pack in a BCT crystal, however this phase is not readily accessible *via* self-assembly. *(E)* An example of the plastic crystal formed by TC. Note that some orientations are more prevalent than others, but long-range orientational order does not exist. *(F)* Compression of the PRC leads to an apparent orientational glass with FCC order wherein particles have one of six distinct orientations. Unlike in a plastic crystal, particles cannot readily change their orientation.

From this, we construct an orientational order parameter (OOP):

$$\Theta = \frac{\Psi_s - \Psi_r}{1 - \Psi_r} . \tag{4}$$

For a crystal with perfect global orientational order, $\Theta = 1$ since for each particle, q will be one of the $q_{\text{ref},j}$ and so $\Psi_s = 1$ by construction. For a crystal with random orientations, $\Theta = 0$.

We use this measure to define how similar, on average, particle orientations within a system are to those of a perfect, dense crystal. This order parameter shares similarities with the frequently used cubatic order parameter[14,18,29,30], but it differs in a few key respects. Most notably, it does not require that the particles have cubic symmetry. In addition, this order parameter does not compare the orientation of all particles against a single, global orientation, an essential feature when investigating structures with multiple orientations in their ordered state, such as the BCT structures of TC and PRC.

We calculate the PMFT to show how the local particle environments depend on particle shape and system density. The PMFT, which we compute with the *freud* software toolbox[31], uses a three-dimensional probability distribution function to determine the free energy associated with a neighboring particle in some position relative to a fixed orientation for a reference particle. Thus, when particles freely rotate among all orientations with an equal probability, there are no preferred locations for neighboring particles relative to the freely rotating reference particle. Isotropic free energy isosurfaces in the PMFT result from such free rotations. When particles adopt preferred relative orientations, *e.g.*, facet-to-facet, an anisotropic PMFT results, revealing the distribution of DEFs[23,24].

To further describe the orientational order present in the particles' local environments, we calculate the relative misorientation of neighboring particles to provide a one-dimensional representation of orientation-orientation coupling for nearest neighbors. We compute the minimum angle required to rotate a particle into an orientation identical to each of its neighbors, and we represent this information as a histogram. The angle separating two orientations is extracted as shown in Eqn. 1; in this process, we account for equivalent orientations based on the point group symmetry of the shapes. By measuring this orientation-orientation coupling, we can identify when neighboring particles tend to align with parallel orientations, when they take on orientations that span specific angles, or when they appear to adopt random orientations with respect to one another.

3 Results

3.1 First-Order Transition

The truncated cuboctahedron (TC) shows a first-order transition from a plastic crystal to a crystal. First-order transitions upon compression of the plastic crystalline phase have been reported for other shapes[16,18]. An apparent hallmark of these transitions is a change in orientational order that coincides with a change in translational order. Here, compression of the TC's pFCC crystal leads to the formation of a BCT structure with two preferred particle orientations in the unit cell. The preferred orientation of the crystal directly determines the unique axis of the simulation box as it undergoes tetragonal symmetry breaking. In the limit of infinite pressure, we expect a denser packing of TC in a single-particle, monoclinic unit cell[32].

The equation of state reveals that the pFCC-to-BCT crystal transition is first order. In *NPT* simulations (the inset in Fig. 3*A*), hysteresis is observed when comparing data obtained upon compression and expansion. For *NVT* simulations, two-phase coexistence and a Mayer-Wood loop[33,34] are observed at the transition from the pFCC to BCT crystal. In the Supplementary Information, we

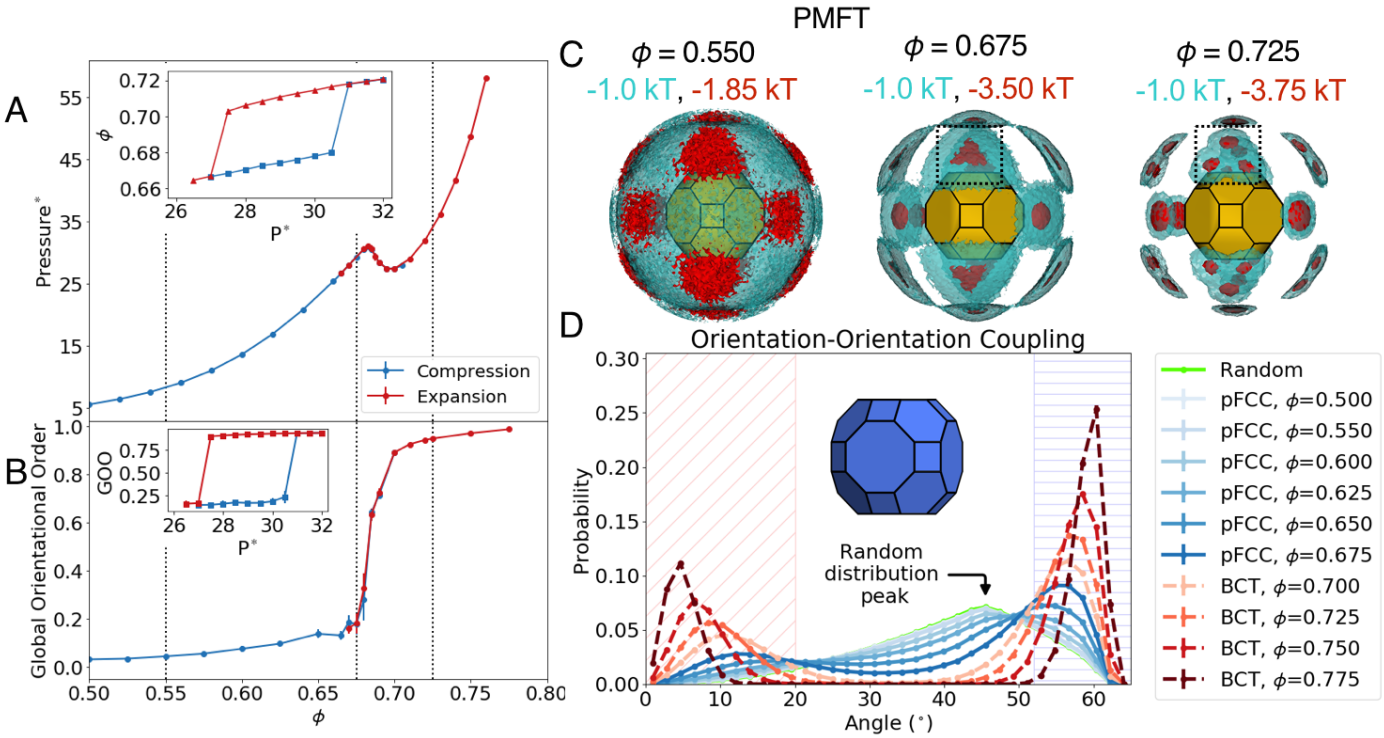

Fig. 3 Phase behavior of the truncated cuboctahedron (TC): first-order phase transition from plastic crystal to crystal. *(A)* The equation of state shows a Mayer-Wood loop in the *NVT* ensemble (main plot) and hysteresis between the pFCC crystal and the BCT crystal in the *NPT* ensemble (inset). Both of these features indicate a first-order transition. *(B)* The orientational order parameter displays a mild increase within the pFCC phase and is significantly higher in the BCT phase; it also exhibits hysteresis in the *NPT* ensemble (inset). *(C)* PMFTs at three state points: as the density increases in the plastic crystal phase ($\phi = 0.550$ & $\phi = 0.675$), the strength of the DEFs increases, but the basic shape persists and the $-1k_BT$ isosurface remains connected. After the transition to a BCT phase ($\phi = 0.725$), the DEF sites at the hexagonal facets split into three unique minima (see dashed-line box), and the $-1k_BT$ isosurface does not connect across the different wells. *(D)* The plot of the orientation-orientation coupling as a function of density shows the development of two peaks. In the BCT crystal, neighboring particles either have similar orientations (separated by $< 20°$, marked with red diagonal lines in the background) or they exhibit a misalignment close to $60°$ (marked with blue horizontal lines in the background). This trend develops in the pFCC phase and strengthens after the transition to the BCT crystal. System sizes $N = 864$ are used for primary plots in (A) & (B), and system sizes $N = 2048$ are used for (C) & (D) along with the insets in (A) & (B).

include a figure that shows the magnitude of the Mayer-Wood loop decreasing with system size and local density comparisons showing the pFCC and BCT phases in coexistence. Further evidence for the first-order nature of the phase transition between pFCC and BCT is given by the observed discontinuity in the first derivative of the OOP with respect to density, showing a clear jump in value between the pFCC and BCT crystal phases. This response in the OOP occurs because of the spontaneous change in the distribution of orientations as the cubic symmetry is broken. Once the system exhibits tetragonal symmetry, the individual particles preferentially adopt just two orientations.

The PMFT likewise displays discontinuous behavior across the transition. The dotted boxes in Fig. 3*C* highlight a change in the shape of the strongest DEF sites across the phase transition. For the TC, the DEF site opposite each hexagonal facet is connected as one continuous isosurface for the pFCC crystal, but it separates into three distinct isosurfaces in the BCT crystal. Within the pFCC phase, increasing the density strengthens the DEFs, but it does not significantly change their shape. The PMFT also reveals that the six octagonal and eight hexagonal facets most frequently align with neighboring particles. These 14 DEF sites do not align with the 12 coordinating neighbors found with FCC positional order.

The orientation-orientation coupling reveals changes in the local particle environments across the phase transition. Fig. 3*D* shows histograms of the minimum angle of misorientation between neighboring particles as a function of density. At low densities (*e.g.*, $\phi \sim 0.50$), neighboring misorientations in plastic crystals follow a random distribution. Because of the particles' rotational symmetry, relative random orientations do not lead to a normal distribution, but rather to a 'sharkfin'-shaped distribution[35]. The sharkfin shape arises because there are more paths to rotate a particle to a symmetrically equivalent orientation for higher misorientation angles. In the BCT phase, one peak develops for small angles corresponding to neighboring particles aligning (marked in Fig. 3*D* with red diagonal hatch lines) and a second peak develops around a larger angle corresponding to particles misaligned in a specific manner (marked with blue horizontal hatch lines). These two peaks begin to develop with increasing density in the pFCC phase, indicating that the local environment in the pFCC adopts features resembling the BCT phase before any long-range, system-wide symmetry breaking occurs.

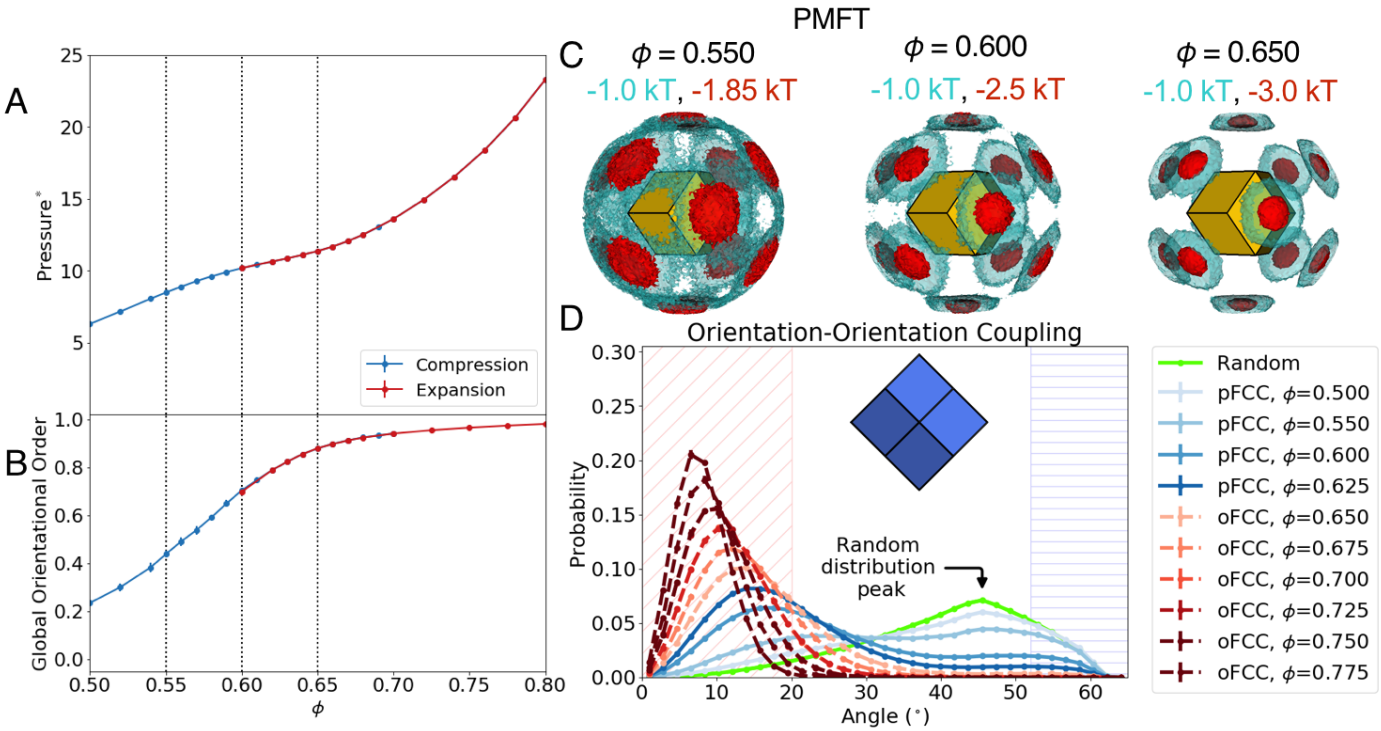

Fig. 4 Phase behavior of the rhombic dodecahedron (RD): gradual order development. *(A)* The equation of state shows no distinct features of a phase transition or dependence on the initial state. *(B)* The global orientational order parameter begins with a value above zero and shows a rapid rise between densities of $\phi = 0.50$ and $\phi = 0.65$ before it begins to converge to 1.0 more slowly. *(C)* At all densities, the strongest DEFs are located at the 12 facets of the RD. The relative spread of the $-1.0k_BT$ isosurface decreases with increasing density while the strength of the primary DEF sites increases. *(D)* Increasing the density of the system results in increasing the likelihood of particles to have progressively similar orientations (region with red diagonal hatch lines), as the likelihood of a large misalignments shows a monotonic decrease (region with blue horizontal hatch lines). System sizes $N = 864$ are used for primary plots in (A) & (B), and system sizes $N = 2048$ are used for (C) & (D).

3.2 Gradual Order Development

The rhombic dodecahedron (RD, see Fig. 4) and the rhombicuboctahedron (RC, see Fig. 5) both show a gradual development of orientational order upon compression of the PC and do not exhibit a sharp thermodynamic transition to a crystal. When in an ordered FCC (oFCC) crystal, both shapes adopt a single orientation, but the development of orientational order is different because of the larger number of facets on the RC (18 square and 8 triangular facets) as compared to the RD (12 identical, rhombic facets). The equations of state for both shapes lack the signature of a first-order transition between PC and crystal phases: they show no hysteresis or coexistence between orientationally ordered and disordered phases. We also found no dependence on system size for the equation of state (see SI), indicating that there is no critical length scale and that the development of orientational order is not a second-order phase transition[36]. For the RD, we note that long-range orientational order develops well before the system is expected to pack at $\phi = 0.80$[37].

While neither shape produces a plastic crystal phase that is thermodynamically distinct from the crystal; we observe that RD and RC systems show plastic crystalline behavior up to densities of approximately $\phi \leq 0.63$ and $\phi \leq 0.70$, respectively; these values are approximate because we cannot define a clear transition point; however, we observe notable differences in behavior above and below these densities. The global orientational order (shown in Figs. 4*B* & 5*B*) distinguishes plastic crystal from crystal behavior. At densities low enough to observe plastic crystal behavior, the OOP increases rapidly with density. After the change from plastic crystal to crystal behavior, the slope decreases as the order parameter tends towards 1.0, *i.e.*, the perfectly ordered value.

The PMFT and orientation-orientation coupling also show characteristics of plastic crystal behavior at intermediate densities. When the system exhibits PC behavior, the PMFT is only weakly anisotropic (see Figs. 4*C* & 5*C*). At the lowest densities, isosurfaces corresponding to DEFs of $-1k_BT$ are continuously connected across all facets, indicating that particle alignments other than facet-to-facet are not strongly penalized and changes in particle orientation are relatively easy. As the density increases, the 12 DEF sites congruent with FCC's coordination environment become increasingly stronger as compared to other arrangements. When this disparity in DEF strength is large enough, PC behavior ceases. The orientation-orientation coupling offers a clearer guideline as to when strong orientational order develops. The strongest feature of Figs. 4*D* and 5*D* is that it becomes increasingly likely for particles to align in parallel as the density increases. Connected with this development is the decreasing probability of non-aligning orientation pairs. To distinguish plastic crystal behavior from crystal behavior in these systems, one can use the density at which the probability of finding intermediate misorientations between particles goes to zero.

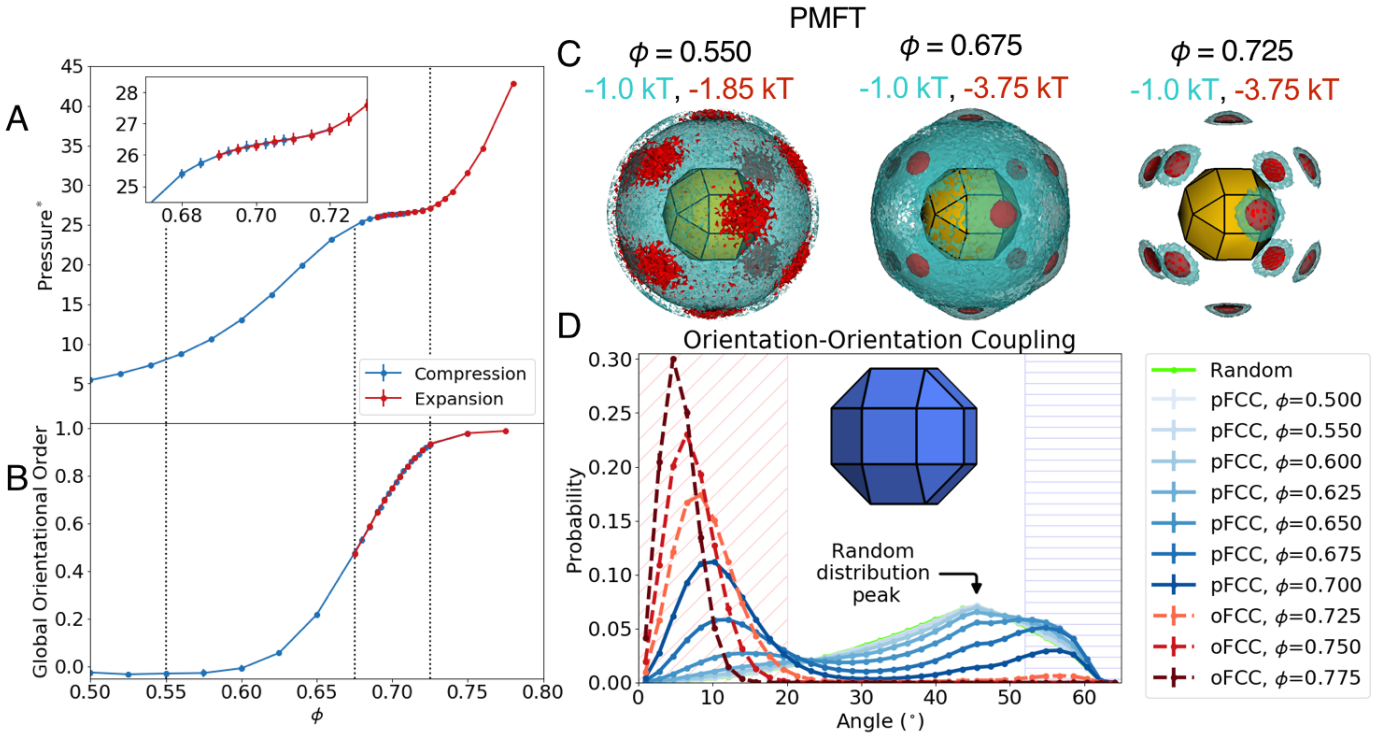

Fig. 5 Phase behavior of the rhombicuboctahedron (RC): gradual order development. *(A)* The equation of state lacks the signature of a first-order transition, although it flattens considerably around a density of $\phi = 0.70$. *(B)* The global orientational order parameter does not increase for densities $\phi < 0.60$, but then begins to display a steady rise. *(C)* The location of the strongest DEF sites remains the same across all densities, although the spread of the $-1.0k_BT$ isosurface is drastically reduced at high densities. *(D)* With increasing density, neighboring particles become more likely to adopt equivalent orientations (region with red diagonal hatch lines). For densities $\phi \leq 0.70$, large misalignments between neighboring particles (*e.g.*, separation angles of $\sim 55°$; marked with blue horizontal hatch lines) occur more frequently than in a random distribution of orientations. System sizes $N = 864$ are used for primary plots in (A) & (B), and system sizes $N = 2048$ are used for (C) & (D) along with the inset in (A).

While there are similarities in the transition behavior for these two shapes, the additional facets in RC lead to plastic crystal behavior occurring over a wider range of densities as compared to RD. In the Supplementary Information, we show the probability of particles adopting specific orientations as a function of density. For both RD and RC, the probability of particles adopting particle orientations corresponding to the oFCC structure monotonically increases with density. However, with RC there are additional orientations that particles adopt at intermediate densities between the fluid and oFCC that occur more frequently than in a random distribution. In contrast, no such trend exists with RD. In a system of RC, the transition from plastic crystal to crystal behavior occurs as the probability of finding these additional orientations rapidly decreases.

Understanding the additional preferential orientations arising when RC displays plastic crystal behavior explains some additional discrepancies between RD and RC in Figs. 4 and 5. The RC equation of state shows a distinctive near-flattening between the densities $0.675 < \phi < 0.725$ (*i.e.*, the inset region of Fig. 5*A*). In this density range, additional preferred orientations vanish from the equilibrium system. In the OOP, the additional orientations suppress the value of the calculated order parameter. In Fig. 5*B*, the value of the OOP remains zero up to a density of $\phi \sim 0.60$. The trend also affects the local environment in the orientation-orientation coupling: when RC exhibits plastic crystal behavior, the probability of finding high-angle misalignments between neighbors is greater than that of a random distribution of orientations (marked with blue horizontal hatch lines in Fig. 5*D*).

3.3 Orientational Glassy Behavior

Systems of pseudorhombicuboctahedra (PRC) form a pFCC crystal that fails, upon further compression, to form a crystal. Through high-pressure simulations with small numbers of particles to probe packing behavior, we found that PRC densely pack in a BCT crystal where the two-particle unit cell contains particles with two orientations. However, upon compression PRC do not spontaneously undergo tetragonal symmetry breaking where two orientations are preferred over all others. The equation of state (shown in Fig. 6*A*) reflects this behavior and shows hysteresis for densities $\phi > 0.72$. When the system is expanded from an initially dense packing, the BCT structure is stable at high densities and begins to transition to FCC around a density $\phi \sim 0.73$. For systems initialized in a pFCC crystal and compressed to higher densities, no phase transition occurs and higher pressures are observed as compared to the BCT-initialized systems. These systems of PRC at high densities with FCC positional order show behavior in line with the approach to an orientational glass[8,10]: particles adopt one of a few distinct orientations and rotational dynamics slow down.

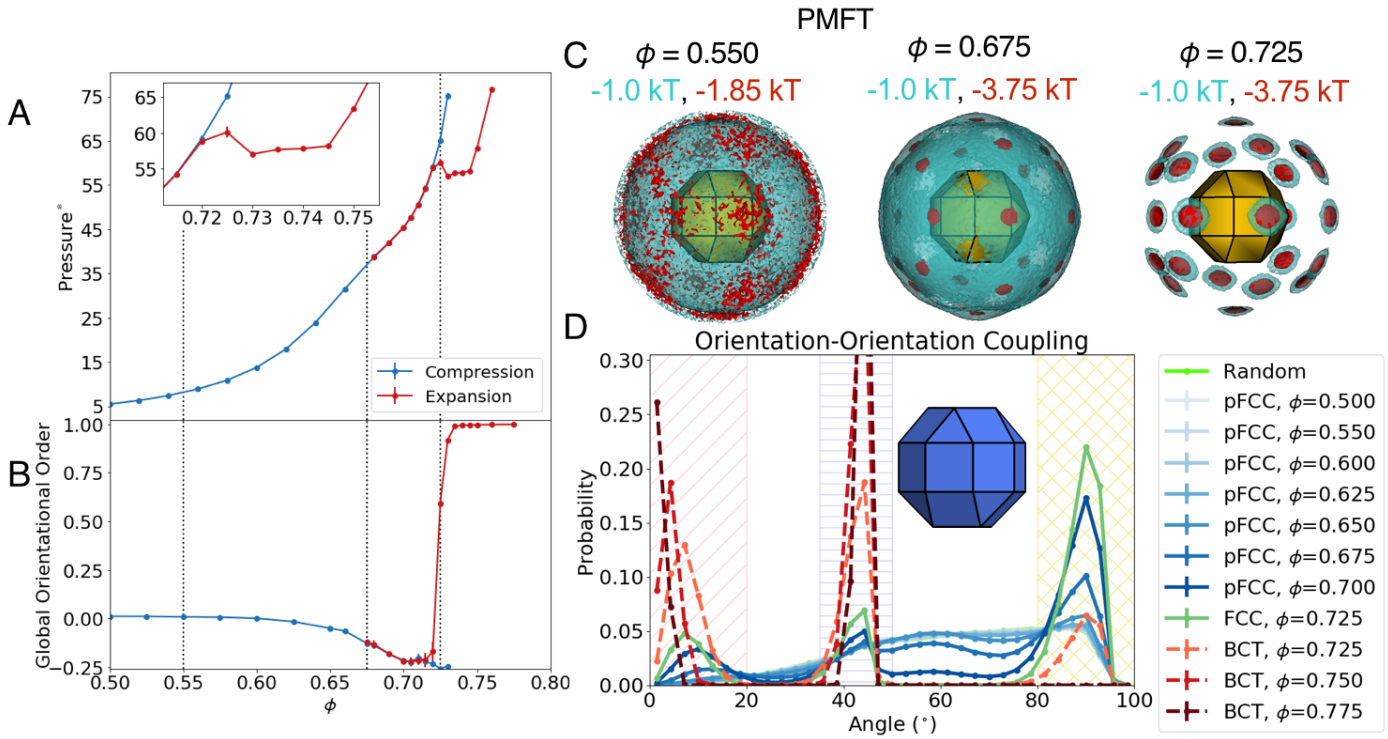

Fig. 6 Phase behavior of the pseudorhombicuboctahedron (PRC): orientationally glassy behavior. *(A)* PRC melt to a pFCC crystal when initialized in the BCT structure and relaxed to lower densities. However, no phase transition occurs when PRC are initialized in a plastic crystal and compressed; FCC translational order persists and particles adopt six orientations in a non-periodic manner. In the BCT structure, particles preferentially adopt two orientations. *(B)* As the density of the plastic crystal increases, the global orientational order parameter goes below zero because particles increasingly adopt one of six separate orientations. In the BCT crystal, the global order is near one because the particles predominantly have just one of two orientations. *(C)* PMFT for pFCC at $\phi = 0.550$ and $\phi = 0.675$ and for BCT at $\phi = 0.725$. At the lowest densities, the PMFT is highly isotropic. At a density $\phi = 0.675$, 24 distinct DEF sites develop, but the $-1k_BT$ isosurface is still relatively isotropic. For the BCT phase at $\phi = 0.725$, the connectivity of this $-1k_BT$ isosurface disappears. *(D)* Upon compression, three distinct peaks develop in the orientation-orientation coupling. The largest peak corresponds to an $\sim 90°$ misalignment in these cases (marked with checkered yellow hatch lines). When the system is initialized in a BCT structure with two types of orientations, the highest peaks correspond to aligning orientations (marked with red diagonal hatch lines) of $\sim 45°$ misalignments (marked with blue horizontal hatch lines). System sizes $N = 864$ are used for primary plots in (A) & (B), and system sizes $N = 2048$ are used for (C) & (D) along with the inset in (A).

The global orientational order of PRC shows a distinctive behavior that is dictated by the particle shape and the apparent transition to an orientational glass. In Fig. 6*B*, the primary result to note is that global order does not develop upon compression of the system. Instead, the OOP becomes negative at densities $\phi > 0.62$. We rationalize this behavior by inspecting the orientations that appear in the BCT packing. The unit cell of the BCT packing contains two particles in an alternating arrangement that are separated by a 45° rotation. The BCT packing can break cubic symmetry along three separate directions, resulting in six distinct orientations. When compressing the system, particles will preferentially adopt one of these six orientations (as can be seen in Fig. 2*F*). Based on how the order parameter is defined in Eqn. 4, the preference towards these six orientations away from a more random distribution leads to a negative value.

Calculation of the misorientations between neighbors in Fig. 6*D* further clarifies the above description of the behavior of the six orientations. In BCT packing, most neighboring particles have orientations separated by less than 20° (*i.e.*, approximately aligned in parallel) or $\sim 45°$ (*i.e.*, alternating orientations compatible with the BCT structure). In the higher-density structures that retain cubic translational symmetry, neighboring particles are approximately four times more likely to be misaligned by $\sim 90°$ than they are to align or adopt the alternating orientation.

The difference in behavior between PRC and RC is clearly illustrated by the PMFTs in Fig. 6*C*. Both shapes have the same numbers and types of facets; however, PRC has a lower point symmetry. One can construct the location of the 24 DEF sites in PRC by duplicating the PMFT of RC and applying a 45° rotation. The PMFT helps us to understand the apparent approach toward an orientational glass: the lower symmetry of PRC leads to many distinct orientations that are comparable from a DEF perspective. By having so many configurations with degenerate free energies, the system is unable to undergo a long-range symmetry breaking wherein particles preferentially adopt one of two orientations as required to transition to a BCT crystal.

4 Discussion

Our analysis of plastic crystal behavior as exhibited by four different systems of hard polyhedra shows that while orientations unsurprisingly become less random with increasing density in all cases, the specifics of order development depend on shape. By

comparing our results for the TC, RD and PRC to the behavior shown by RC, we can connect how specific features of particle shape affect phase behavior.

When measuring the global orientational order for systems with arbitrary symmetry, a comparison against the orientation(s) that appear in the denser, orientationally ordered phase is paramount. When a system gradually develops orientational order, measures of global orientational order also increase gradually as the particles progressively adopt the ordered orientation. In these cases, the transition away from PC behavior can roughly be defined by the flattening of the measure of global orientational order with respect to density (see Figs. 4*B* & 5*B*) as it subsequently approaches 1.0, *i.e.*, the fully ordered state. When the plastic crystal is a distinct thermodynamic phase, global measures of orientational order will exhibit a jump at the transition as global symmetry is broken.

Descriptors of the local environment appear to be effective at distinguishing whether or not orientational order develops. We characterized local environments *via* the PMFT and by computing orientation-orientation coupling between neighboring particles based on relative angles of separation. These two descriptors capture information about orientational order development, but express it in slightly different ways. In terms of the PMFT (which expresses the effective free energy of different pair configurations), the loss of plastic crystal behavior occurs when the PMFT shows high free energies between the primary DEF sites. The orientation-orientation coupling leads to a similar conclusion: the loss of plastic crystal behavior and development of long-range orientational order corresponds to densities where the misorientation angle probability for intermediate configurations vanishes.

This work can be seen as an extension of previously identified rules for the orientational order in two-dimensional systems of hard polygons[21]. Polygons that possess the same symmetry as the two-dimensional lattice into which they crystallize are found not to display a distinct plastic crystal phase. On the other hand, shapes that share a subset of symmetry elements with their lattice will exhibit a plastic crystal with preferred polygon orientations. These exact rules do not hold in three dimensions because particle symmetry does not dictate faceting – and thus DEFs – in the same way (*e.g.*, RC and TC have identical symmetry, but due to different faceting, their PMFTs show 12 and 14 DEF sites, respectively). Instead, one must compare the alignment of a shape's largest facets to its crystal environment to arrive at similar rules.

TC provides an example where the DEFs set by the facets do not align with the coordination geometry set by the translational order of the plastic crystal. When in the pFCC phase, shapes such as TC must inherently have equivalent facets pointing in different directions while maintaining the cubic symmetry. These systems can show a few distinct, preferred orientations within the plastic crystal; for TC there are three such orientations. As the density increases and systems are driven toward configurations that pack more effectively, the TC particles break the cubic symmetry and preferentially adopt two orientations associated with the BCT crystal.

When DEFs do align with the crystal coordination, order develops gradually without a distinct phase transition. In these cases, it is possible for each individual particle to adopt an orientation wherein a facet is turned in the direction of each neighbor. For the case of FCC crystal structures with a cuboctahedron-shaped coordination polyhedron, the shape must have large facets characteristic of the rhombic dodecahedron (the dual of the cuboctahedron). For lower-density crystals, it is unlikely for long-range orientational order to exist because there are still many other orientations that are accessible. As the density increases, more and more particles adopt the orientation that maximizes alignment of the largest facets on neighboring particles, and long-range order develops as a result. Comparison of RD and RC shows that decreasing the relative size of the coordination-aligned facets will delay the development of long-range orientational order.

The final case studied possesses a subtle tweak to the facet symmetry because of the gyrated nature of the PRC. While the RC contains a single, symmetrically distinct orientation that maximizes facet-to-facet alignment of neighbors in an FCC environment, systems of PRC become orientationally frustrated upon an increase in density, and the resulting configuration contains six orientations compared with the expected two in an ideal BCT structure. Long-range order fails to develop because there are too many distinct particle arrangements that are all entropically very similar. Instead, entropy favors orientational degeneracy at the lower densities, and once the density is high enough where packing arguments would favor the orientationally ordered BCT over a disordered FCC arrangement, rotational dynamics have slowed down to where order cannot develop anymore. A similar argument has been made related to the Voronoi particle of the lonsdaleite (hexagonal diamond) structure type[38].

5 Conclusion

In this work, we investigated four systems of hard polyhedra that exhibit the characteristic behavior of plastic crystals: translational order, but orientational disorder. The behavior in these systems was studied through equations of state, global order measures, and local environment measures. We showed that orientational order can develop with increasing density in three ways. A plastic crystal can undergo a first-order phase transition when long-range orientational order develops along with a concomitant change to the translational order. Plastic crystals can undergo other transitions that are not distinct, thermodynamic transitions. They can gradually develop long-range orientational order without a change in translational order, or they can rotationally vitrify, wherein translational order does not change and particles become stuck in a few distinct but random orientations.

The behavior of these systems can most readily be understood through the lens of the theory of directional entropic forces[22–24]. When plastic behavior occurs in a system of hard particles, DEFs will show some preferences, but the entropic forces are not too strongly anisotropic. If DEFs align with a crystal's coordination geometry, order can be expected to gradually develop. If the DEFs show there to be many equivalent arrangements, the system will likely fail to develop long-range orientation order. Otherwise, the misalignment between a particle's DEFs and the crystal's coordination geometry will result in first-order transitions. Figure 7

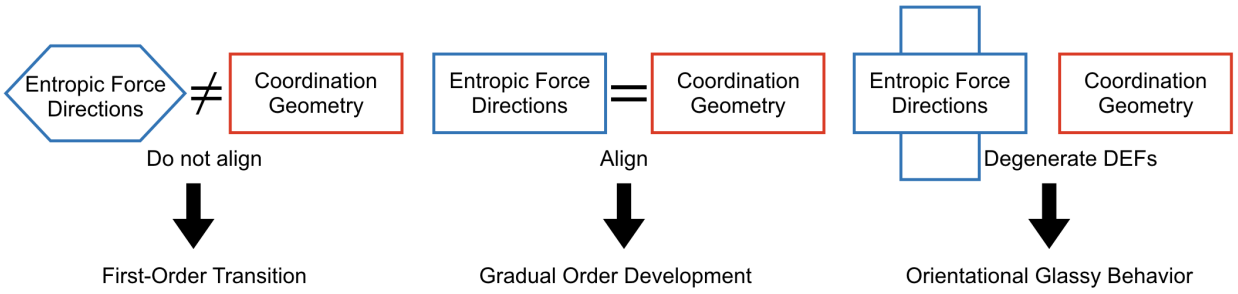

Fig. 7 Summary of the design rules established in this work. The alignment between the directional entropic forces (which are set by particle shape) and the coordination geometry (which is set by the structure) dictates the freezing transition when a plastic crystal is compressed. First-order transitions, gradual order development, and orientational glassy behavior are all possible with the compression of a plastic crystal.

summarizes the the different plastic crystal transitions that result from the possible relationships between DEFs and coordination geometry.

Our findings can be used toward more general design of plastic crystal properties in anisotropic colloidal systems. If the facets of a particle are not congruent with the local environment in a plastic crystal, then a first-order transition (and the hysteretic behavior that comes with it) can be expected upon changing the density (or pressure) of a system. If one desires to achieve a more continuous control over the orientational order, then a building block with facets that do align with a crystalline environment will be necessary. The relative size of the coordination-aligned facets presents a design knob with these cases of gradual order development: plastic crystal behavior can be accentuated and allowed to occur over a wider range of pressures or densities by using smaller facets. Lastly, while small tweaks to particle shape can change the lattice for a densest packing, an actual phase transition can be inaccessible because of degeneracy in the ensuing DEFs of the lower-symmetry shape.

6 Acknowledgments

We thank E.S. Harper, C.X. Du, and R.K. Cersonsky for fruitful discussions. This material is based upon work supported in part by the U.S. Army Research Office under Grant Award No. W911NF-10-1-0518 and also by a Simons Investigator award from the Simons Foundation to Sharon Glotzer. J.D. acknowledges support through the Early Postdoc Mobility Fellowship from the Swiss National Science Foundation, grant number P2EZP2_152128. This research was supported in part through computational resources and services supported by Advanced Research Computing at the University of Michigan, Ann Arbor, and it used the Extreme Science and Engineering Discovery Environment[39] (XSEDE), which is supported by National Science Foundation grant number ACI-1053575; XSEDE award DMR 140129.

Notes and references

1 D. Frenkel, *Computer Physics Communications*, 1987, **44**, 243–253.
2 F. M. van der Kooij and H. N. W. Lekkerkerker, *The Journal of Physical Chemistry B*, 1998, **102**, 7829–7832.
3 H. Kikuchi, M. Yokota, Y. Hisakado, H. Yang and T. Kajiyama, *Nature Materials*, 2002, **1**, 64–68.
4 L. Pauling, *Physical Review*, 1930, **36**, 430.
5 J. Timmermans, *J. Chim. Phys.*, 1938, **35**, 331–344.
6 J. Timmermans, *Journal of Physics and Chemistry of Solids*, 1961, **18**, 1–8.
7 *The Plastically Crystalline State*, ed. J. N. Sherwood, John Wiley & Sons, Ltd., 1979.
8 H. Suga and S. Seki, *Journal of Non-Crystalline Solids*, 1974, **16**, 171–194.
9 R. Brand, P. Lunkenheimer and A. Loidl, *Journal of Chemical Physics*, 2002, **116**, 10386–10401.
10 C. Talón, M. A. Ramos and S. Vieira, *Physical Review B*, 2002, **66**, 1–4.
11 O. Yamamuro, H. Yamasaki, Y. Madokoro, I. Tsukushi and T. Matsuo, *Journal of Physics: Condensed Matter*, 2003, **15**, 5439–5450.
12 J.-M. Meijer, A. Pal, S. Ouhajji, H. N. W. Lekkerkerker, A. P. Philipse and A. V. Petukhov, *Nature Communications*, 2017, **8**, 14352.
13 H. R. Vutukuri, A. Imhof and A. Van Blaaderen, *Angewandte Chemie - International Edition*, 2014, **53**, 13830–13834.
14 U. Agarwal and F. A. Escobedo, *Nature Materials*, 2011, **10**, 230–5.
15 P. F. Damasceno, M. Engel and S. C. Glotzer, *Science (New York, N.Y.)*, 2012, **337**, 453–7.
16 R. Ni, A. P. Gantapara, J. de Graaf, R. van Roij and M. Dijkstra, *Soft Matter*, 2012, **8**, 8826.
17 A. P. Gantapara, J. de Graaf, R. van Roij and M. Dijkstra, *Physical Review Letters*, 2013, **111**, 015501.
18 A. P. Gantapara, J. de Graaf, R. van Roij and M. Dijkstra, *The Journal of Chemical Physics*, 2015, **142**, 054904.
19 A. K. Sharma, V. Thapar and F. A. Escobedo, *Soft Matter*, 2018, **14**, 1996–2005.
20 M. Burian, C. Karner, M. Yarema, W. Heiss, H. Amenitsch, C. Dellago and R. T. Lechner, *Advanced Materials*, 2018, 1802078.
21 W. Shen, J. Antonaglia, J. A. Anderson, M. Engel, G. van Anders and S. C. Glotzer, *Soft Matter*, 2019, **15**, 2571–2579..
22 P. F. Damasceno, M. Engel and S. C. Glotzer, *ACS Nano*, 2012, **6**, 609–14.
23 G. van Anders, N. K. Ahmed, R. Smith, M. Engel and S. C.

Glotzer, *ACS Nano*, 2014, **8**, 931–40.
24 G. van Anders, D. Klotsa, N. K. Ahmed, M. Engel and S. C. Glotzer, *Proceedings of the National Academy of Sciences*, 2014, **111**, E4812–E4821.
25 J. A. Anderson, C. D. Lorenz and A. Travesset, *Journal of Computational Physics*, 2008, **227**, 5342–5359.
26 J. Glaser, T. D. Nguyen, J. A. Anderson, P. Liu, F. Spiga, J. A. Millan, D. C. Morse and S. C. Glotzer, *Computer Physics Communications*, 2015, **192**, 97–107.
27 J. A. Anderson, M. E. Irrgang and S. C. Glotzer, *Computer Physics Communications*, 2016, **204**, 21–30.
28 L. Filion, M. Marechal, B. van Oorschot, D. Pelt, F. Smallenburg and M. Dijkstra, *Phys. Rev. Lett.*, 2009, **103**, 188302.
29 J. A. C. Veerman and D. Frenkel, *Phys. Rev. A*, 1992, **45**, 5632–5648.
30 P. D. Duncan, M. Dennison, A. J. Masters and M. R. Wilson, *Phys. Rev. E*, 2009, **79**, 031702.
31 E. S. Harper, M. Spellings, J. Anderson and S. C. Glotzer, *Zenodo. https://doi.org/10.5281/zenodo.166564*, 2016.
32 E. R. Chen, D. Klotsa, M. Engel, P. F. Damasceno and S. C. Glotzer, *Phys. Rev. X*, 2014, **4**, 011024.
33 J. E. Mayer and W. W. Wood, *The Journal of Chemical Physics*, 1965, **42**, 4268–4274.
34 J. A. Anderson, J. Antonaglia, J. A. Millan, M. Engel and S. C. Glotzer, *Phys. Rev. X*, 2017, **7**, 021001.
35 J. K. Mason and C. A. Schuh, *Acta Materialia*, 2009, **57**, 4186–4197.
36 N. Goldenfeld, *Lectures On Phase Transitions And The Renormalization Group (Frontiers in Physics)*, Addison-Wesley, 1992.
37 R. K. Cersonsky, G. van Anders, P. M. Dodd and S. C. Glotzer, *Proceedings of the National Academy of Sciences*, 2018, **115**, 1439–1444.
38 B. A. Schultz, P. F. Damasceno, M. Engel and S. C. Glotzer, *ACS Nano*, 2015, **9**, 2336–2344.
39 J. Towns, T. Cockerill, M. Dahan, I. Foster, K. Gaither, A. Grimshaw, V. Hazlewood, S. Lathrop, D. Lifka, G. Peterson, R. Roskies, J. Scott and N. Wilkins-Diehr, *Computing in Science Engineering*, 2014, **16**, 62–74.